

ACCELERATED CHARGING OF PCM IN HORIZONTAL LATENT HEAT STORAGE UNIT USING DIFFERENT MULTITUBE ARRANGEMENT

Digant S. Mehta*, Manish K. Rathod, Jyotirmay Banerjee

Department of Mechanical Engineering, Sardar Vallabhbhai National Institute of Technology (SVNIT), Surat, GUJARAT, INDIA

ABSTRACT

Practical use of Latent Heat Storage Unit (LHSU) is limited due to poor thermal conductivity of Phase Change Material (PCM). Present research is focused on acceleration of the charging process of LHSU using different arrangement of HTF tubes. Numerical analysis is reported for estimation of thermal performance of horizontal shell and tube type latent heat storage unit using multiple HTF tubes. In the present study stearic acid (melting point 55.7°C -56.6°C) is used as PCM. Results infer significant augmentation of charging rate for multiple HTF tubes. However, highest charging rate is obtained for those cases where more HTF tubes are placed below the diametric plane of horizontal LHSU.

Keywords: Shell and tube, Latent Heat Storage Unit, Phase Change Material, Multitube.

Nomenclature

A_{mush}	Mushy zone constant
δ	Liquid fraction
\bar{S}	Source term
t	Time (s)
T	Temperature of PCM (°C)
\vec{V}	Velocity vector (m/s)
	Subscripts
$T_{solidus}$	Solidus temperature (°C)
$T_{liquidus}$	Liquidus temperature (°C)

1. INTRODUCTION

Solar thermal energy is the most appropriate alternative to meet the energy demands of tropical country like India. However, for better use of solar energy, there is a need to develop storage system which

stores the solar energy during sunshine hours and the same energy can be retrieved during non-sunshine hours. Latent Heat Storage Units (LHSU) using Phase Change Materials (PCMs) is an attractive way to store thermal energy. Such devices store/retrieve energy by phase change of PCMs from solid to liquid and vice-versa.

The performance of any LHSU depends on the heat transfer mechanisms involved in the LHSU. However, low thermal conductivity of PCMs (0.15 W/mK to 0.3 W/mK) affects the phase transition rate [1] and slows down the energy storage/retrieval rate. Thus, it is necessary to devise mechanisms which accelerate the charging and discharging of the PCM. This can be achieved by employing extended surfaces (fins), thermal conductivity enhancement using nanoparticles and metal foams, multiple PCM methods and micro-encapsulation [2]. Mechanism of heat transfer can also be altered by change in orientation [3] or change in the eccentricity [4] of Heat Transfer Fluid (HTF) pipe.

Charging and discharging of the PCM can also be achieved by use of HTF tubes in multi-tube arrangement [5–12]. However, only few researches [9,11,12] have analysed charging and discharging process using different arrangement of the HTF tubes. In the present research, influence of multi-tube (single HTF tube, 3 HTF tubes, and 4 HTF tubes) arrangement on charging characteristics of horizontal LHSU is analysed numerically.

2. PHYSICAL MODEL AND NUMERICAL METHODOLOGY

2.1 PHYSICAL MODEL

Fig. 1 (a) shows the shell and tube type heat exchanger with single HTF tube considered for the present research. It consists of two concentric cylinders of length 600 mm. The inside tube of 28 mm inner diameter and 30 mm outer diameter is made of brass. The outside tube of inner diameter 88 mm and outer diameter 92 mm is made of stainless steel. Different multi-tube arrangement considered for augmentation of heat transfer are shown in Fig. 1(b), (c), (d), (e), (f), (g).

Diameter of each tube is chosen in a such a way that total PCM area (= 0.0054 m²) is not altered[12]. The geometric dimensions for different cases are listed in the Table 1. Stearic acid is used as a PCM. Melting point and latent heat of stearic acid are determined using the Differential Scanning Calorimeter (DSC). Thermo-physical properties of stearic acid and water (HTF) are listed in Table 2.

$$\frac{\partial}{\partial t}(\rho H) + \nabla \cdot (\rho \vec{V} H) = \nabla \cdot (k \nabla T) \quad (3)$$

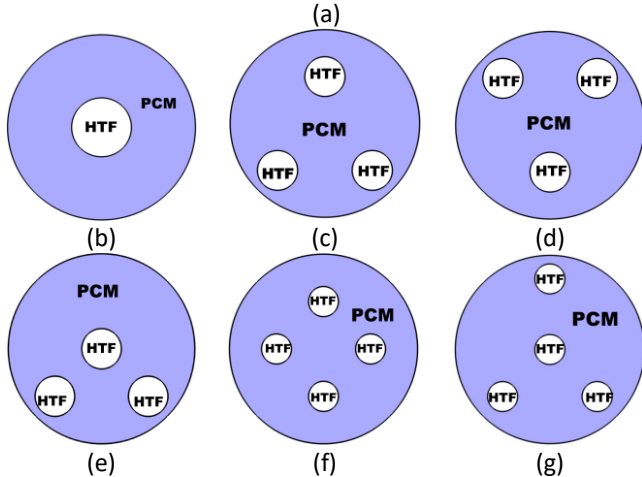


Fig 1 (a) Physical model of horizontal LHSU (b) Case I (c) Case II (d) Case III (e) Case IV (f) Case V (g) Case VI

TABLE 1 GEOMETRIC DIMENSIONS FOR DIFFERENT CASES

CASE	Internal dia. of shell (mm)	Inner dia. of HTF tubes (mm)	PCM area (m ²)
I	88	28	0.0054
II, III, IV	88	17	0.0054
V, VI	88	14	0.0054

TABLE 2 THERMOPHYSICAL PROPERTIES OF STEARIC ACID

Melting point (°C)	55.7-56.6
Latent heat (kJ/kg)	196.1
Density (kg/m ³)	Solid-960 Liquid-840
Specific heat (J/kg K)	Solid-3000 Liquid-2100
Thermal conductivity (w/m K)	Solid-0.3 Liquid-0.172
Coefficient of thermal expansion (1/K)	0.0001
Dynamic viscosity (kg/m s)	0.00772

2.3 INITIAL AND BOUNDARY CONDITIONS

In the present model, the outer wall is modelled as adiabatic wall and the inner surface of the HTF wall is subjected to convective heat flux boundary condition corresponding to forced convection heat transfer from the HTF fluid. The heat transfer coefficient is calculated as[14]:

$$h = Nu \frac{k}{D} \quad (4)$$

$$Nu = \frac{\left(\frac{f}{8}\right)(Re-1000)Pr}{1 + 12.7\left(\frac{f}{8}\right)^{\frac{1}{2}}\left(Pr^{\frac{2}{3}} - 1\right)} \quad (5)$$

where Pr is the Prandtl number and Re is the Reynolds number expressed by

$$Re = \left(\frac{4\dot{m}}{\pi D \mu}\right) \quad (6)$$

f is the friction factor and is calculated as:

$$f = (1.58 \ln Re - 3.28)^{-2} \quad (7)$$

The PCM is initially set as solid at a temperature of 28°C. Results are reported for HTF flow of 5 kg/min. The inlet HTF temperature is maintained at 85°C for melting process.

2.4 VALIDATION OF THE NUMERICAL MODEL WITH EXPERIMENT

2.2 NUMERICAL METHODOLOGY

Phase change phenomena is analysed using enthalpy-porosity formulation [13] available in ANSYS-FLUENT 16. In this approach, liquid fraction indicates the fraction of the cell volume that is in liquid state. The liquid fraction is computed at each iteration based on an enthalpy balance. The temperature of PCM is obtained by iteration between the energy equation and the liquid fraction equation. Moreover, the enthalpy-porosity technique treats the mushy region as a porous medium. The porosity in each cell is set equal to the liquid fraction in that cell. In fully solidified regions, the porosity is equal to zero setting velocity to be zero in these regions. The momentum source term in the mushy zone takes the following form:

$$\vec{S} = \frac{(1-\delta)^2}{(\delta^3 + \varepsilon)} A_{mush} \vec{V} \quad (1)$$

Liquid fraction is computed as

$$\delta = 1 \text{ if } T > T_{liquids}, \delta = 0 \text{ if } T < T_{solidus}$$

$$\delta = \frac{T - T_{solidus}}{T_{liquids} - T_{solidus}} \text{ if } T_{solidus} < T < T_{liquids} \quad (2)$$

The numerical results obtained in the present study for 2-D horizontal configuration is compared with the experimental results obtained from our in-house experimental test facility for horizontal shell and tube type LHSU configuration shown in Fig 2(a). PCM average temperature shown in Fig. 2 (b) depicts good agreement between experimental and numerical (2D and 3D) results. In horizontal LHSU, temperature variations remains identical in the axially. Thus, 2D slice has chosen to reduce the computational time.

3. RESULTS AND DISCUSSION

Fig. 3 shows liquid fraction contours of PCM for different cases during the charging process at different time intervals. In each case computed liquid fraction is labelled for different time interval. In each case, initially a small thin layer of PCM is formed around HTF tube. Conduction mode of heat transfer is dominant in the initial phase of change process. Amount of molten PCM is not adequate in order to build natural convection current. As time elapses, more molten PCM is formed and natural convection current is established above the HTF surface. This enables circulation of hot molten PCM above the HTF surface. Charging rate is faster for case I (Single concentric HTF tube) up to a time period of 120 minutes. The liquid fraction computed at this time is 0.6789. It depicts that more than half of the PCM mass is charged. The natural convection current is set up only in the upper half of diametric plane. The dominant mode of heat transfer is conduction in the lower half. As a result, the process of phase change is very slow once the upper half is completely molten. It is observed from Fig. 3 that during time period of 120 minutes and 180 minutes, the computed liquid fraction changes from 0.6789 to 0.8411 by 180 minutes. The entire charging process is completed by 310 minutes depicting that 190 minutes is required for computed liquid fraction to reach from 0.6789 to 1. Thus, for acceleration of charging process, it is required to enhance the charging rate of the PCM specifically in the bottom half of the LHSU. This can be achieved by circulation of the molten PCM more uniformly in the LHSU.

To achieve uniform rate of heat transfer for the entire charging process, arrangement of the multiple HTF tubes is proposed such that charging in the lower diametric plane of LHSU can be improved. Fig. 3 (b) to (f) show liquid fraction contours for the different multi-tube arrangements (Case- II to VI). No significant difference in the computed liquid fraction is noticed between the

different cases initially up to 30 minutes. However, at same time, the liquid fraction estimated for the LHSUs having 4 HTF tubes is lower than that for cases with 3 HTF tubes.

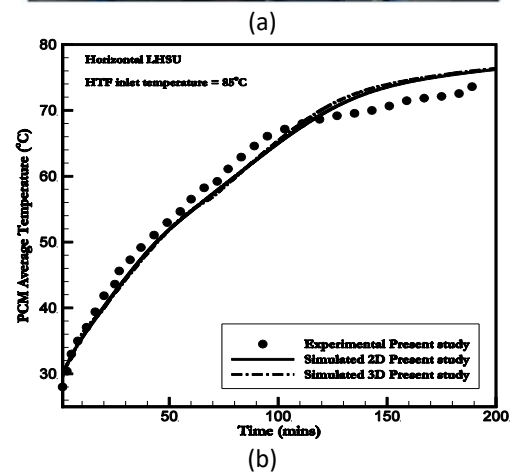
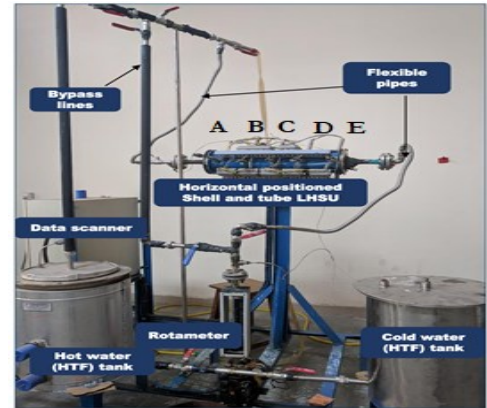


Fig 2 (a) Experimental test setup (b) Comparison of numerical results with present experiments

This is because of lesser area available for natural convection of molten PCM for more number of HTF tubes. As time advances to 60 minutes, faster charging occurs for the case II and IV due to larger area available for convective heat transfer above the HTF surface. For case III, charging of the PCM increases gradually.

As time advances to 120 minutes, highest liquid fraction is noted for case II and IV where charging of the PCM is almost completed ($\delta = 0.9963$ and $\delta = 0.9929$) by this time. A marginal difference in the liquid fraction between case III and IV is due to the fact that in case IV the HTF tubes are being positioned at the lower half of diametric plane of LHSU. At time of 180 minutes, charging of PCM for the cases III and V is not complete. This is owing to the fact that the strength of the natural convection is not adequate as only one tube is positioned in the bottom region. Thus, multi-tube arrangement decides strength of the natural convection which leads to faster charging.

Acceleration of charging is thus obtained by proper positioning the HTF tubes. Results clearly infer that charging is faster for cases where HTF tubes are positioned in the region below the diametric plane. This is also depicted in Fig. 4 which shows the charging time

and percentage reduction in the charging time for the case II to VI as compared to case I. Case IV represents least time for charging of PCM which shows 59.29 % reduction in the charging time where 32.58% reduction in the charging time is noted.

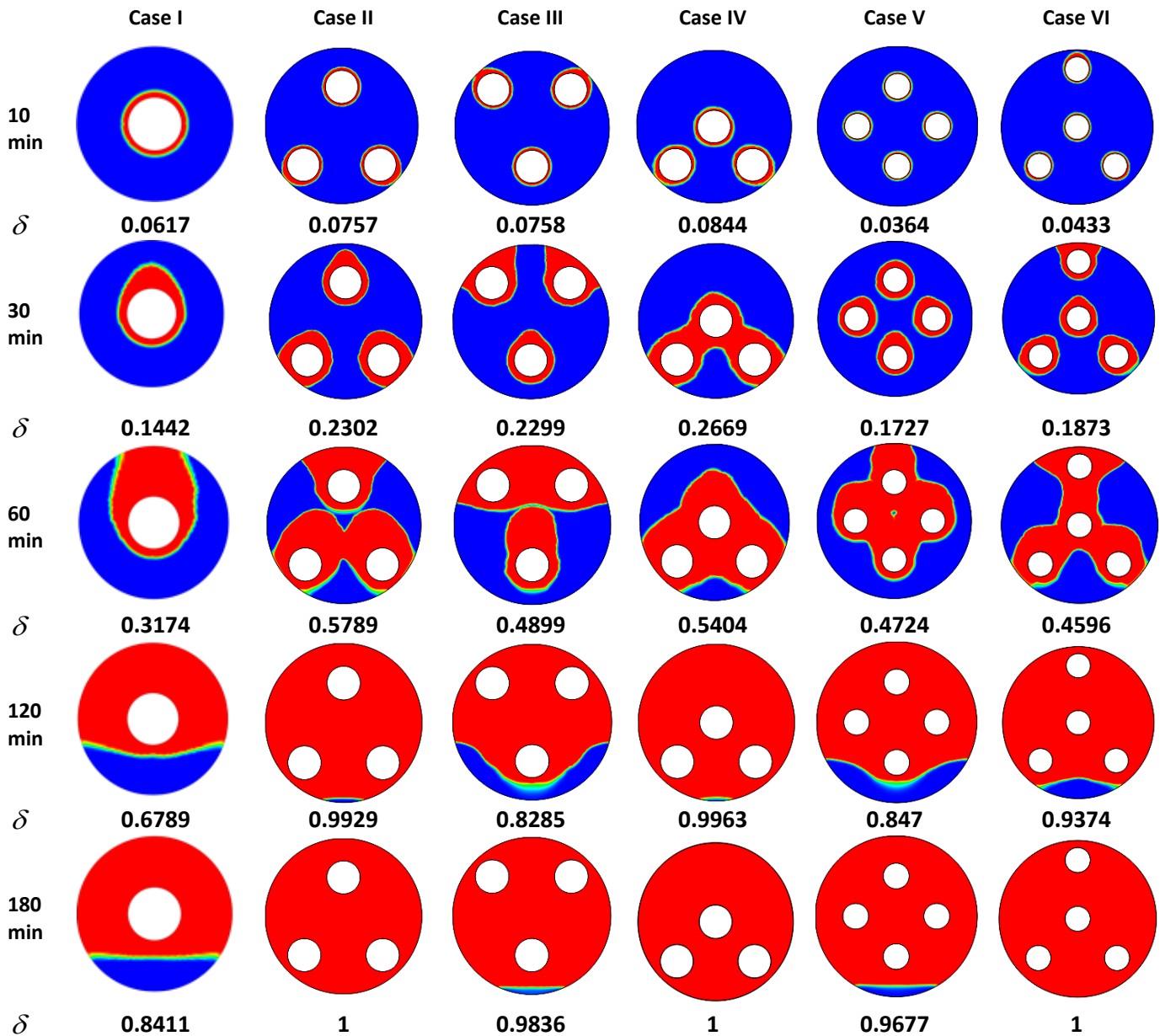


Fig. 3 Contours of liquid fraction for different cases (along with computed liquid fraction)

4. CONCLUSION

Following conclusions have derived from the present study.

- Natural convection plays a significant role during the charging of the PCM.

- Proper arrangement of multi HTF tube provides significant reduction in the charging time for all cases.
- From the present LHSU configurations, charging occurs rapidly in the LHSUs where HTF tubes are positioned in the bottom half of diametric plane.

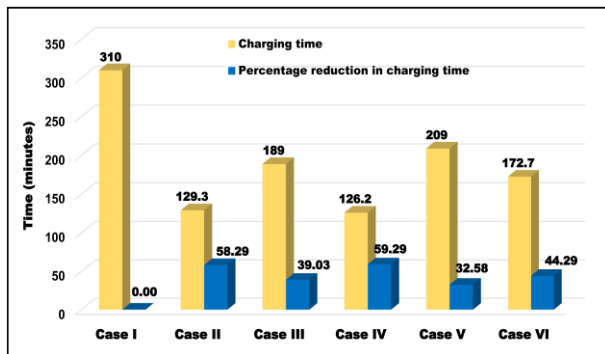


Fig. 4 Comparison of charging time and percentage reduction in the charging time for different cases

REFERENCE

- [1] Rathod MK, Banerjee J. Thermal performance enhancement of shell and tube Latent Heat Storage Unit using longitudinal fins. *Applied Thermal Engineering* 2015;75:1084–92. doi:10.1016/j.applthermaleng.2014.10.074.
- [2] Ibrahim NI, Al-Sulaiman FA, Rahman S, Yilbas BS, Sahin AZ. Heat transfer enhancement of phase change materials for thermal energy storage applications: A critical review. *Renewable and Sustainable Energy Reviews* 2017;74:26–50. doi:10.1016/j.rser.2017.01.169.
- [3] Mehta DS, Solanki K, Rathod MK, Banerjee J. Thermal performance of shell and tube latent heat storage unit : Comparative assessment of horizontal and vertical orientation. *Journal of Energy Storage* 2019;23:344–62. doi:10.1016/j.est.2019.03.007.
- [4] Mehta DS, Vaghela B, Rathod MK, Banerjee J. Heat transfer intensification in horizontal shell and tube latent heat storage unit. *Numerical Heat Transfer, Part A: Applications* 2019;0:1–20. doi:10.1080/10407782.2019.1599273.
- [5] Esen M, Ayhan T. Development of a model compatible with solar assisted cylindrical energy storage tank and variation of stored energy with time for different phase change materials. *Energy Conversion and Management* 1996;37:1775–85. doi:10.1016/0196-8904(96)00035-0.
- [6] Esen M, Durmus A, Durmus A. Geometric design of solar-aided latent heat store depending on various parameters and phase change materials. *Solar Energy* 1998;1:19–28.
- [7] Agyenim F, Eames P, Smyth M. Heat transfer enhancement in medium temperature thermal energy storage system using a multitube heat transfer array. *Renewable Energy* 2010;35:198–207. doi:10.1016/j.renene.2009.03.010.
- [8] Raul AK, Bhavsar P, Saha SK. Experimental study on discharging performance of vertical multitube shell and tube latent heat thermal energy storage. *Journal of Energy Storage* 2018;20:279–88. doi:10.1016/j.est.2018.09.022.
- [9] Jourabian M, Farhadi M, Rabienataj Darzi AA. Accelerated melting of PCM in a multitube annulus-type thermal storage unit using lattice Boltzmann simulation. *Heat Transfer - Asian Research* 2017;46:1499–525. doi:10.1002/htj.21286.
- [10] Bhagat K, Prabhakar M, Saha SK. Estimation of thermal performance and design optimization of finned multitube latent heat thermal energy storage. *Journal of Energy Storage* 2018;19:135–44. doi:10.1016/j.est.2018.06.014.
- [11] Kousha N, Rahimi M, Pakrouh R, Bahrampoury R. Experimental investigation of phase change in a multitube heat exchanger 2019;23:292–304.
- [12] Pourakabar A, Rabienataj AA. Enhancement of phase change rate of PCM in cylindrical thermal energy storage. *Applied Thermal Engineering* 2019;150:132–42. doi:10.1016/j.applthermaleng.2019.01.009.
- [13] Voller VR, Prakash C. A fixed grid numerical modelling methodology for convection-diffusion mushy region phase-change problems. *International Journal of Heat and Mass Transfer* 1987;30:1709–19. doi:10.1016/0017-9310(87)90317-6.
- [14] Incropera FP, Dewitt DP, Bergman TL, Lavine AS. *Fundamentals of Heat and Mass Transfer*, 6th Edition Hoboken, New Jersey, US, Wiley, 2006